AIAC-2013-022

DESIGNING A ROBOTIC FLAPPING WING MECHANISM IN ORDER TO MIMIC THE INSECT FLIGHT

Alper GÜNGÖR[1], Talha MUTLU[2] and Dilek Funda KURTULUŞ[3],

Middle East Technical University
Ankara, TURKEY

ABSTRACT

Insect flight fascinates the scientist and engineers for centuries with the better aerodynamic performance and increased maneuverability. With the recent advances in micro-technologies, it is possible to miniaturize the air vehicles to the size of a bird or an insect. Flapping flight is the most promising technology for the micro air vehicles (MAVs), having maximum weight of 90 gr and dimension of 15 cm [McMichael, 1996]. This paper presents the design and technical futures of dual robotic flapping wing mechanism (Robot-Wings) for use in laboratory experiments, such as aerodynamic performance of different wings, optimization of flapping trajectories. The mechanism is scaled by means of Reynolds number and reduced frequency. There exist two wings which can flap with the maximum angular velocity of 290deg/s and which have a maximum half-span of 20cm. Each wing has three rotational degrees of freedom, which allows the adjustment of different flapping trajectories separately. Six computer-controlled brushless motors drive the three rotational axis of each wing, which are equipped with sensors for measuring the instantaneous aerodynamic forces. A special software and graphic user interference (GUI) are developed for the Robot-Wings. The main objective of the software is to solve the coupled kinematic of the three rotation axes in order to obtain the desired motion trajectories. Hardware of each wing embedded with three motor position readers, three custom made motor control circuits and a microcontroller unit. Different motion trajectories were tested such as pure and combined pitch, plunge and yaw cases. Flow field around the wings will be quantified as a future work by using Particle Image Velocimetry (PIV) technique.

Nomenclature

A	=	amplitude, degree
D	=	offset, degree
K_p	=	P – Constant
T	=	period, s
t	=	timescale, s
x	=	pitch axis
y	=	plunge axis
z	=	yaw axis
α	=	pitch angle, degree
β	=	plunge angle, degree
θ	=	yaw angle, degree
$\dot{\alpha}$	=	pitch rate, degree/s
$\dot{\beta}$	=	plunge rate, degree/s
ε	=	position error
$\dot{\theta}$	=	yaw rate, degree/s
φ	=	phase difference
ζ	=	motion function
ψ	=	PWM signal

Subscripts

e	=	experimental position
d	=	desired position
m	=	motor
w	=	wing

[1]Undergraduate Student in Electrical and Electronics Engineering Department, Email: e174105@metu.edu.tr
[2]Graduate Research Assistant in Aerospace Engineering Department, Email: talha.mutlu@gmail.com
[3]Assoc. Prof. in Aerospace Engineering Department, Email: funda.kurtulus@gmail.com

INTRODUCTION

Recent advances in the microelectronics technology enables the production of smaller UAV systems that are called Micro-UAV. However, MAVs need different lift generating mechanisms rather than fix wing and rotary wing. MAVs that are using flapping flight technologies exhibit superior characteristic compared to fixed wing and rotary wing due to better aerodynamic performance, maneuverability at low flight velocities. There are three main mechanism for extra lift generation during flapping flight. Firstly, dynamic stall of the wing creates strong leading edge vortex (LEV) [Dickinson, 1993], second is the wake capturing phenomenon [Birch, 2003], and the last one is the clap-and-fling mechanism for the tandem wing cases [Weis-Fogh, 1973]. Robotic flapping mechanism presented in this paper, which is instrumented with load and torque sensors, makes possible the investigation of lift-generating mechanisms. Robot-Wings has two independent wings that enables to create different flapping trajectories composed of sinusoidal, step and ramp functions.

The design of the Robot-Wings is originated from three experimental flapping wing setup (Figure 1). First one is the Robofly of the Dickinson Lab. [Dickinson,1993], which is one of the most outstanding experimental setup. It has three rotational degrees of freedom and one degrees of freedom in the flight direction (Figure 1a&b). Another mechanism, which has two rotational degrees of freedom and one degree of freedom in the flight direction is the Robotic Model Wings of Purdue University Bio-Robotic Lab.[Zheng, 2009] (Figure 1c), and the last one is the differentially driven flapping wing mechanism which has three rotational degrees of freedom for each wing [George, 2012] (Figure 1d).

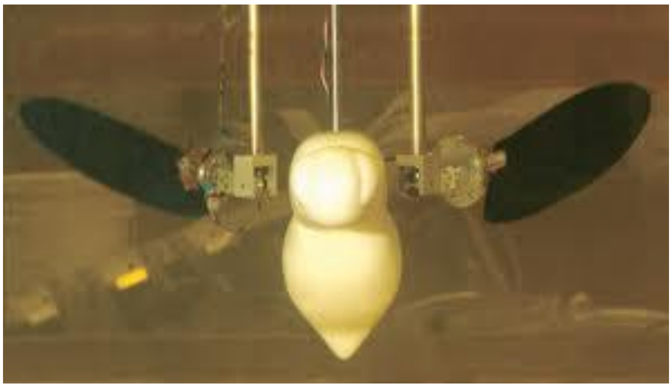

a) Robofly with a scaled model of wasp (Front view)

b) Robofly side view

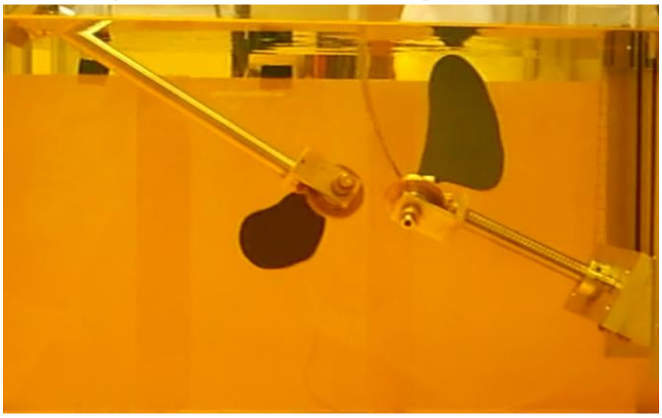

c) Robotic Robot Wings

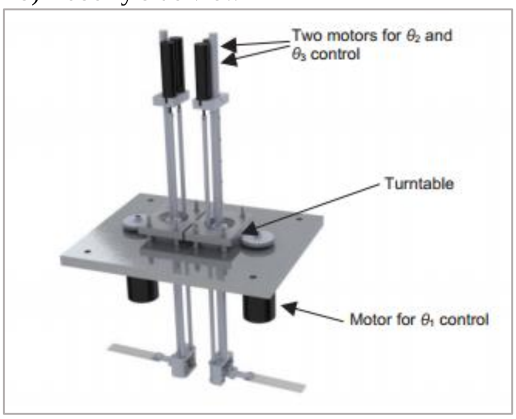

d) Differentially driven flapping wing

Figure 1 Competitor flapping wing test setups [Dickinson, 1993; Zheng, 2009; George, 2012]

SYSTEM DESIGN

Robot-Wings is designed to mimic the flapping wing motion (Figure 2). Each wing can perform plunge, pitch and yaw motion around the x, y and z-axes (Figure 2-b). Rotation by θ around the z-axis is referred to yaw angle; rotation by β around the y-axis is referred to pitch angle; and rotation by α around the x-axis is referred to plunge angle. Wings are capable of performing flapping motion in different mediums such as air, water and oil. Compact gear-box design minimized the flow distribution around the wing. Lift and Drag force can be measured via load cells that are placed between wing and gear-box. Size of the system is determined by means of Reynolds number and reduced frequency.

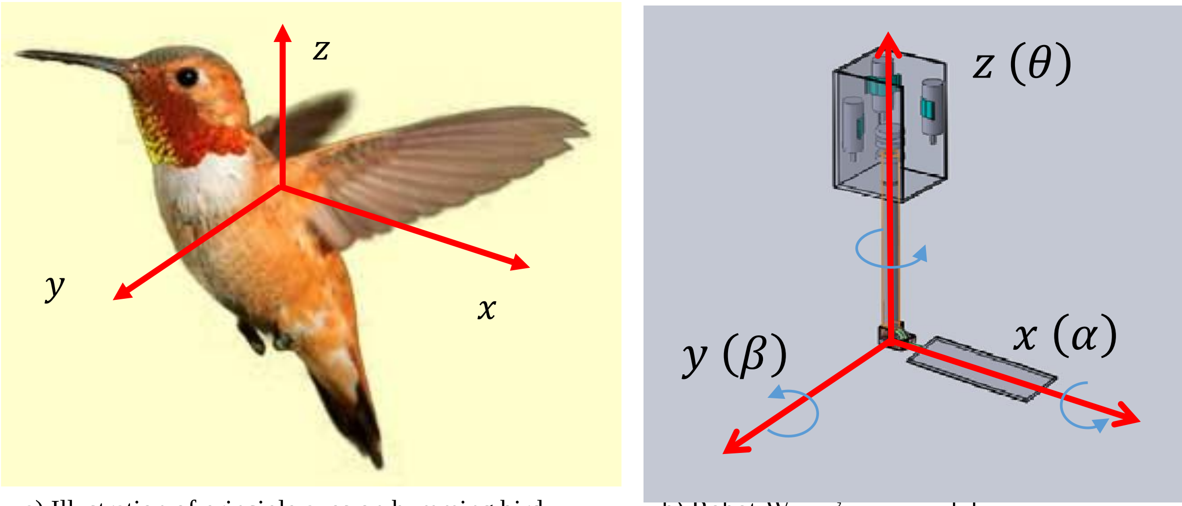

a) Illustration of principle axes on humming bird b) Robot-Wings' wing module

Figure 2 Hummingbird and Robot-Wings principle axes placement

Robot-Wings is capable of performing arbitrary flapping trajectories with six-degree-of-freedom. Position and velocity limits at each axis are presented in Table1.

Table 1 Robot-Wings motion limits

	with Load Cell	*without Load Cell*
α	$\pm 90^0$	$\pm 180^0$
β	$+45^0/-90^0$	$+45^0/-225^0$
θ	$\pm 180^0$	$\pm 180^0$
$(\dot{\alpha})_{max.}$	$160^0/s$	
$(\dot{\beta})_{max.}$	$290^0/s$	
$(\dot{\theta})_{max.}$	$290^0/s$	

Mechanism

Robotic Flapping Wing Mechanism has two identical wing modules. Each wing module has a load cell in order to measure instantaneous lift and drag forces. Wing modules are connected to Control-Box. The system Composed of two wing module and one control-box. It can be connected to PC via USB or RS-232 cable (Figure 3).

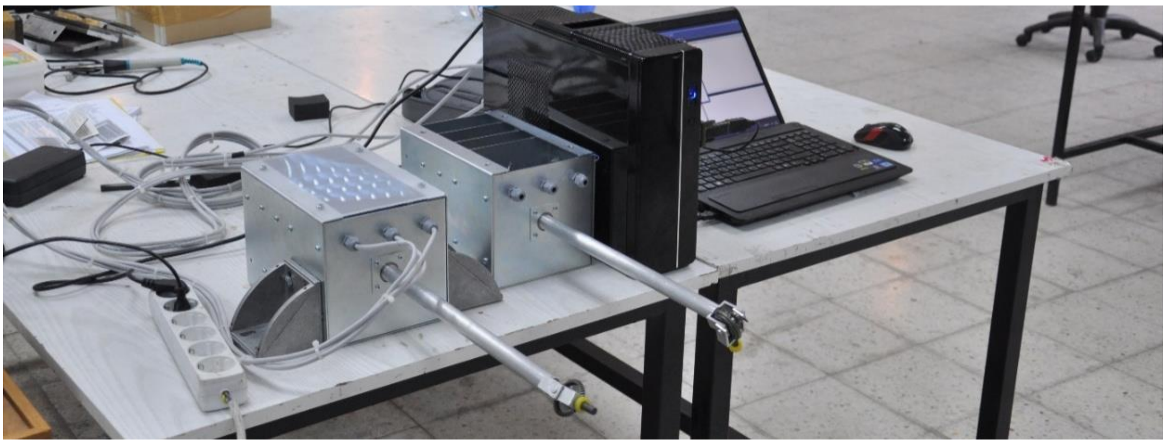

Figure 3 Two wing module and Control-Box

Gear-Box was the most challenging part of the design due to lack of suitable off-the-shelf gears. The current design is similar to the Robofly [Dickinson, 1993]. Figure 4 shows the CAD-drawing, produced gear-box and the gears.

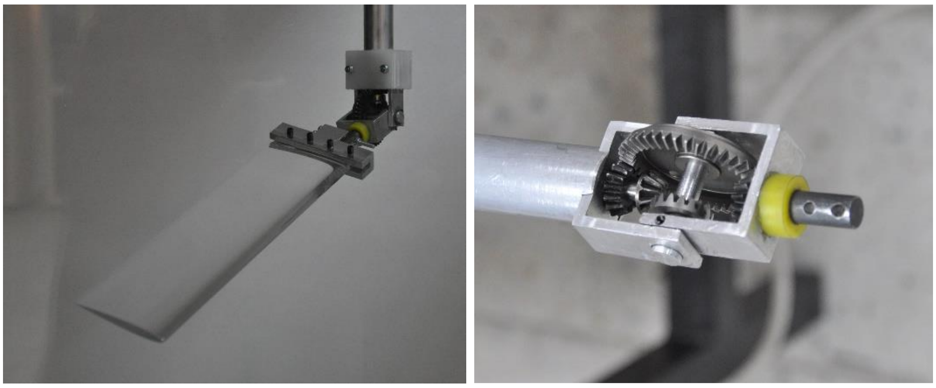

Figure 4 Gear-Box

Six brushless DC motors with integrated encoders were used to actuate the each DOF of the system. The Robot-Wing is designed to use with water tank or tunnel, also it is possible to use the mechanism with wind tunnel. The mechanism mounted on top of the 80x80x200 cm water tank (Figure 5).

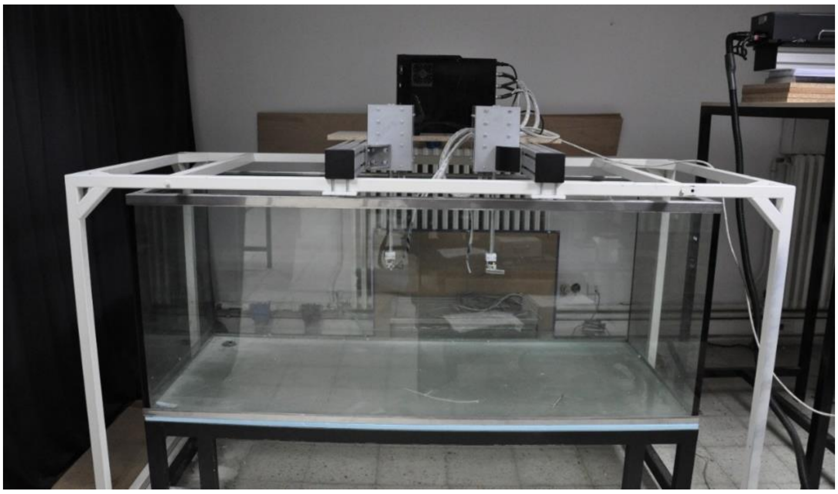

Figure 5 Robot-Wings placed on top of the water tank

A software called Wing Simulator (Wing-Sim) were developed in order to operate Robot-Wings. Experiment cases can be saved to the internal memory within the control-box. Initial position of the wings can be arranged before the experiment and wings automatically return the initial position after the experiment is completed. Type of the function that defines the flapping frequency can be chosen as sine, ramp or step function. Amplitude, period, offset, phase difference, delay and the motion duration can be specified for each wing independently (Figure 7).

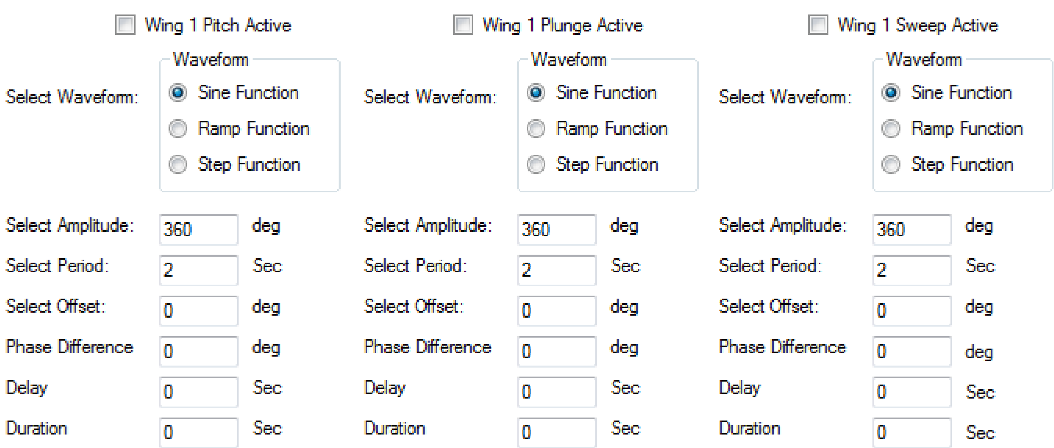

Figure 6 Wing Simulator motion adjustment

Motion Kinematics

Wing-Sim calculates the motor positions in order to obtain the desired wing motions. Axes motions can be defined in three different form – sine, ramp and step functions – by means of amplitude, period, offset, phase difference, delay and duration. Sinusoidal function that defines the wing motions is given below.

$$\zeta_{w,sine}(A, D, T, \varphi, t) = A * \sin(2\pi t/T + \varphi) + D \qquad \text{(Eq. 1)}$$

Each wing capable of performing three motions, namely pitch, plunge and yaw motions by using three electric motors. Motion transmission between wing and motor provided by toothed belt, transmission shaft and gear-box. A conversion matrix between motor motion and wing motion is used due to gear ratios and coupled axes motions.

$$\begin{bmatrix} -1 & -3.308 & 1 \\ 0 & -1.8 & -1 \\ 0 & 0 & 1 \end{bmatrix} \begin{bmatrix} \alpha_w \\ \beta_w \\ \theta_w \end{bmatrix} = \begin{bmatrix} \alpha_m \\ \beta_m \\ \theta_m \end{bmatrix} \qquad \text{(Eq. 2)}$$

$$[A] \begin{bmatrix} \alpha_w \\ \beta_w \\ \theta_w \end{bmatrix} = \begin{bmatrix} \alpha_m \\ \beta_m \\ \theta_m \end{bmatrix} \qquad \text{(Eq. 3)}$$

Pitch axis is not coupled with other axes. On the other hand, plunge axis is coupled with pitch axis and yaw axis is coupled with both pitch and plunge axis. In other words, generating a pure pitch motion only requires using pitch motor, while generating a pure yaw motion requires using all three motor at the same time (Figure 8).

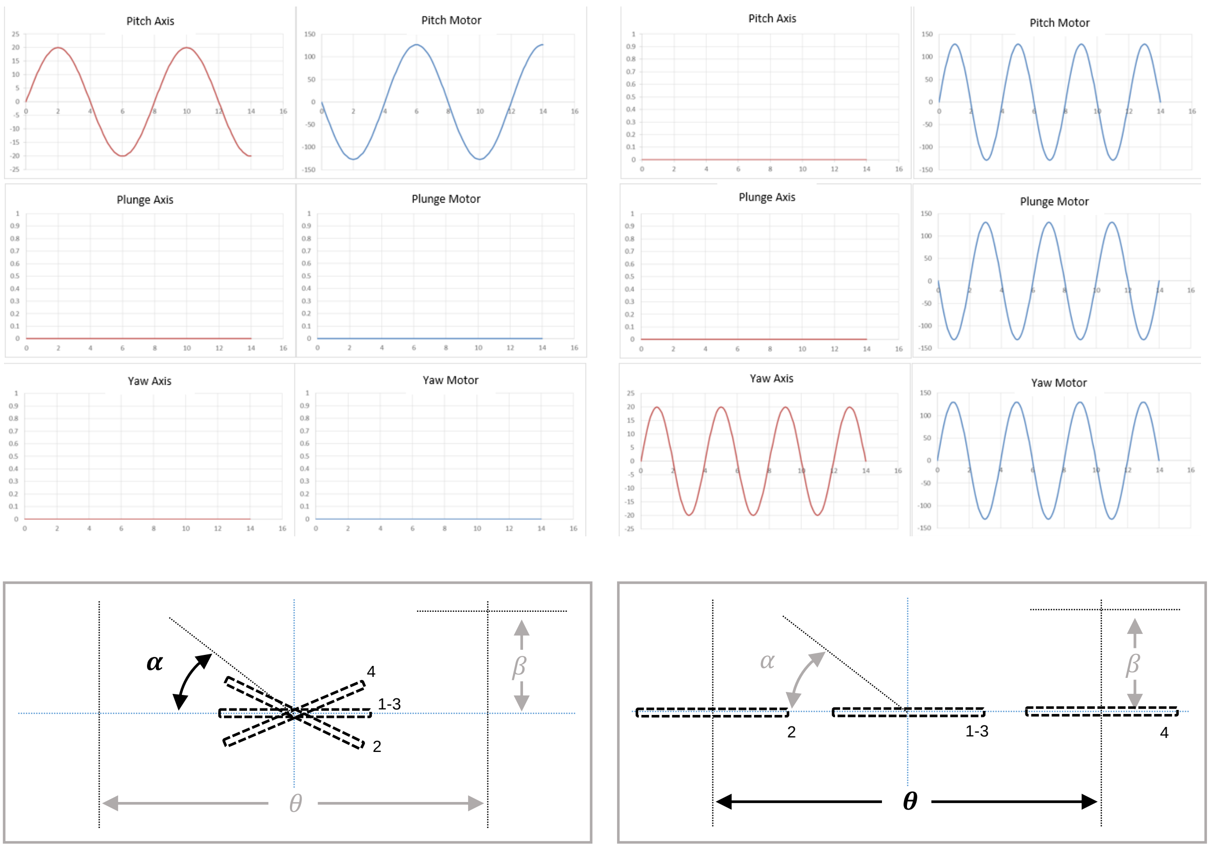

a) Pure pitch motion b) Pure yaw motion

Figure 7 Motor input signals for pure pitch and pure yaw motions

Simultaneous use of two or three axes require much complicate motor motion. Figure 9 shows figure-eight motion with variable pitch and constant pitch angle. While pitch and plunge axis performing simple sinusoidal motions, pitch and plunge motors perform much complex combined sinusoidal motions as seen in Figure 9-a. Although, pitch axis do not move in Figure 9-b, pitch motor still continue to perform complex motion due to coupling of the axes.

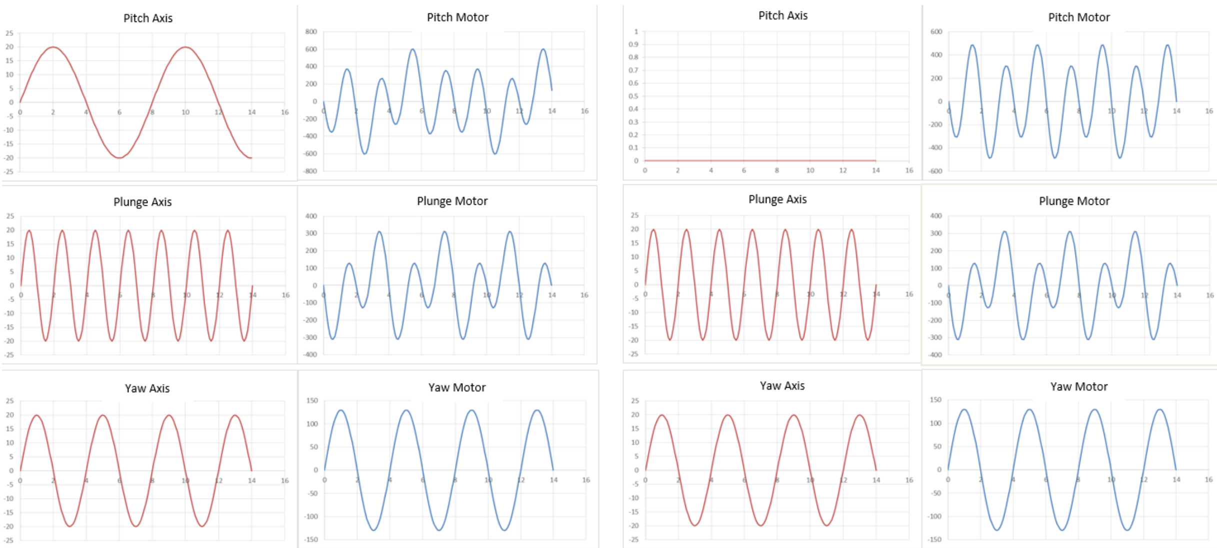

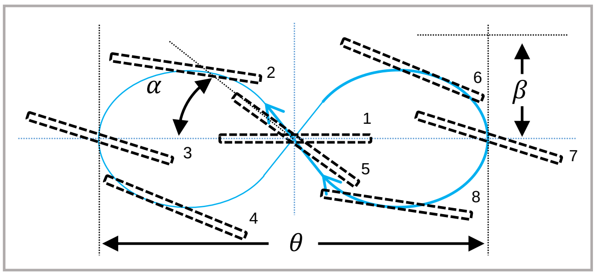

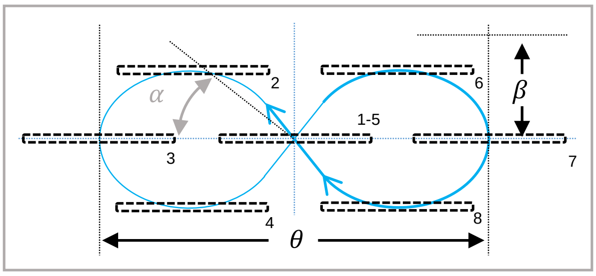

a) Variable pitch angle b) Constant pitch angle

Figure 8 Figure-eight motion

Hardware & Software Development

The Mechanism has two wings, and three custom made MAXON motors, position reader and motor drivers for each wing. Two microcontroller circuits, which are placed in to a control box, are used to control the wings (Figure 9). Wing-Sim, which is a special software created for the Robot-Wings, calculates the necessary motor motions for user defined wing motions. This is done by multiplying a pre-calculated motor Position-coupling matrix with the position vector of the wing axes. The resulting vector is the position vector of the motors. These values are sent to microcontrollers constantly throughout the system runtime since the memory of the microcontroller is limited. The computer also takes the feedback from the microcontroller (motor positions), converts it to axes positions (multiplying by a pre-calculated motor-decoupling matrix). After that, Wing-Sim plots the both desired and experimental position of the each axis on the screen simultaneously. Hence, wing motions can be watched during the experiment. Besides that, after the experiment is done, the Wing-Sim also saves the output in excel format and prints graphics of “experimental positions vs. time” and “desired positions vs. time”. Hence, position data can be investigated after the experiment.

PIC16F777 microcontroller is chosen since it has 3 PWM outputs to control the 3 motors. Position data of each motor is read by microcontroller via position readers. Wing motions are controlled by using position feed-back and desired position values. P- Controller (Proportional Controller) is used to control the motions. Position errors of the axes are calculated during the motion continuously. A PWM response is created for each motor accordingly to position errors. The position reader consists only of a single PIC16F628A. It just reads encoder data of one motor and sends the value to microcontroller when requested. Motor Driver is an integrated circuit that was developed for the mechanism. It can drive one motor in two direction up to 2.5 A and 12 V.

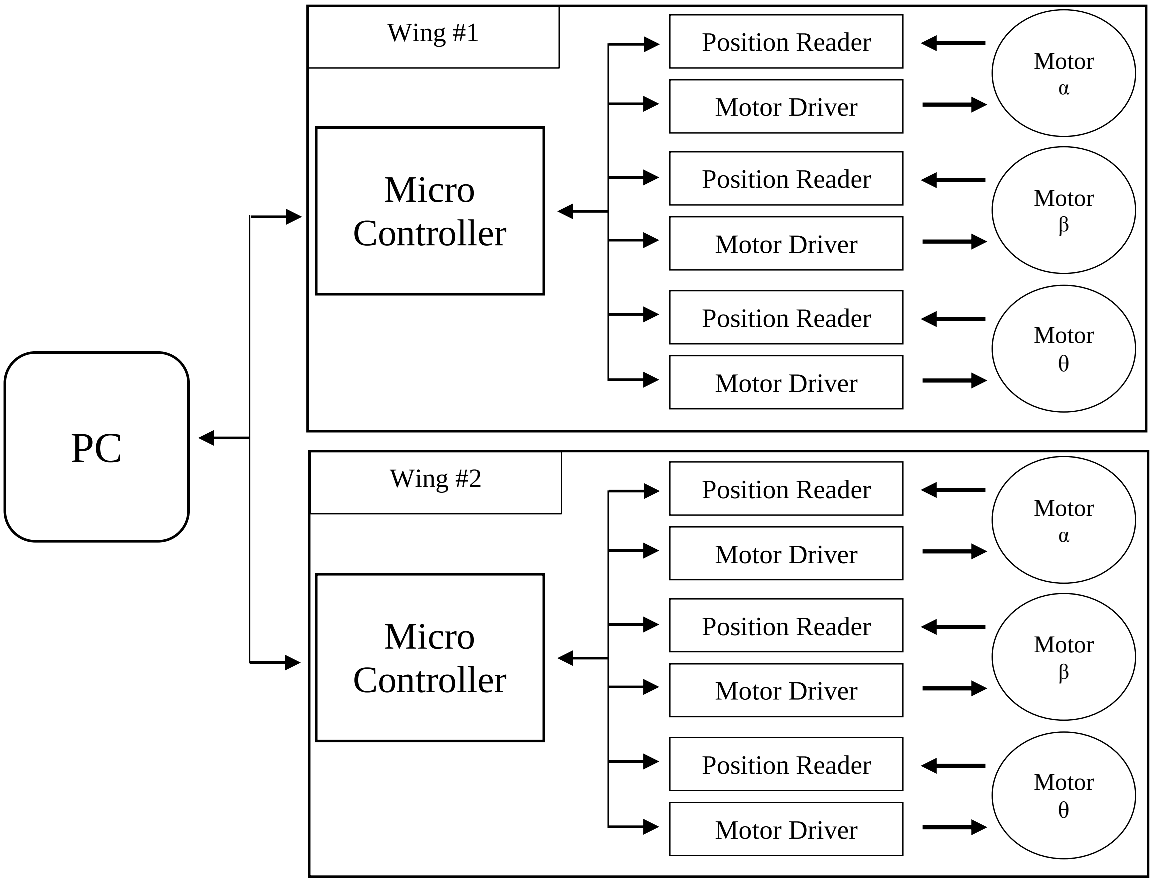

Figure 9 Hardware block diagram

Since microcontroller must know the desired positions at every instant, it is not an option to wait for new data while the motors are active. Therefore, two buffers are used for each motor. Each time the motor starts using data of one buffer, the computer starts sending the other data buffer. Therefore the control is never interrupted and the microcontroller always knows where the motors are expected to be. The communication algorithm is shown in Figure 10.

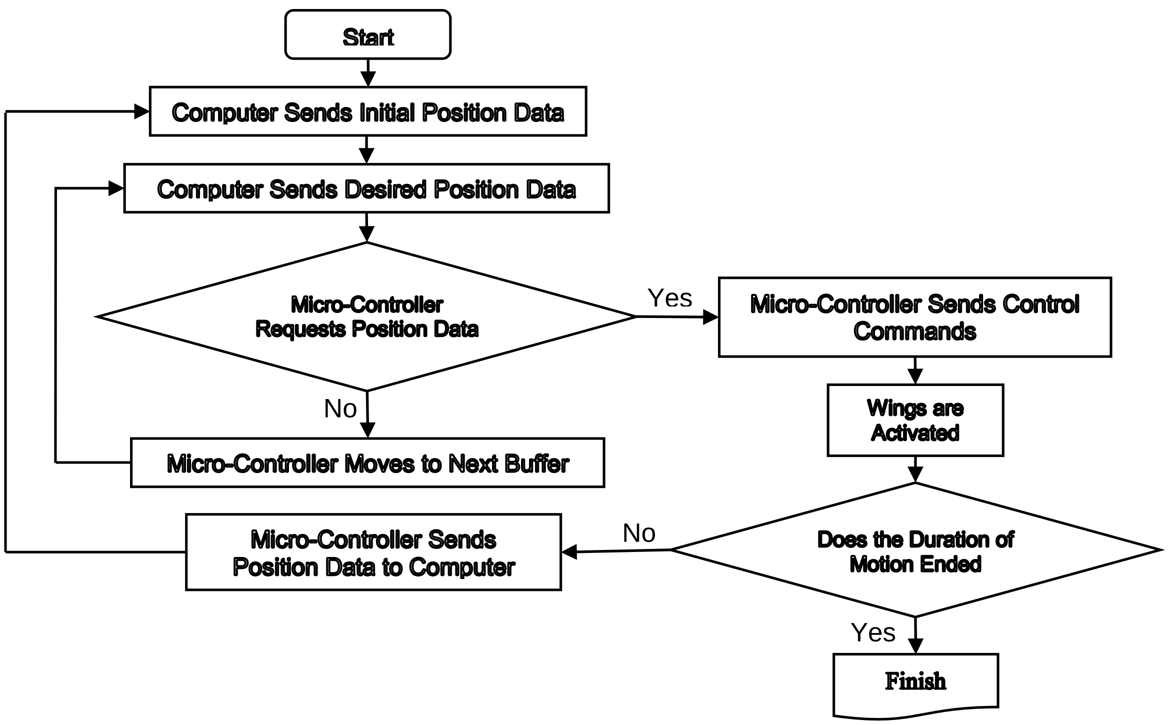

Figure 10 Communication flow chart

P – Constant for each motor was determined experimentally. Each motor should able to overcome aerodynamic or hydrodynamic force generated by the wing and friction force between the gears and shafts. System requires different P – constant calibration for different operational mediums such as water, oil and air. Proportional controller give nearly perfect system responses for large angle values. However, it couldn't compensate the small values. Therefore, it was necessary to use a piecewise function for the Pulse-Width Modulation (PWM) outputs. If the error goes below a certain ε_1 value, PWM stays constant at a minimum PWM value. It is also necessary to define a stability condition. If the error goes below another threshold value and practically becomes zero, PWM signal simply decays to zero. (Figure 11)

$$\psi(\varepsilon) = \begin{matrix} 0 & , & \varepsilon \le \varepsilon_0 \\ \psi_1 & , & \varepsilon \le \varepsilon_1 \\ K_p\varepsilon & , & \varepsilon > \varepsilon_1 \end{matrix} \qquad \text{(Eq. 4)}$$

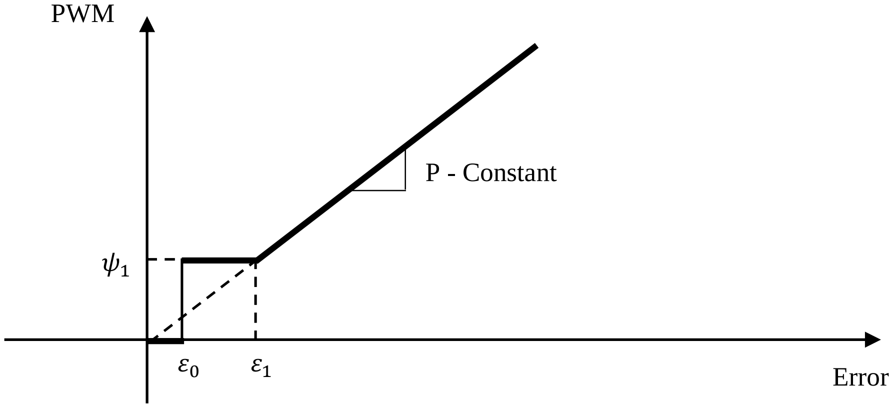

Figure 11 PWM signal versus position error

RESULTS AND DISCUSSION

Robot-wings require special calibration for different experimental environments and wing models. Wing calibration can be done by means of two main parameters. These parameters are P – Constant and minimum PWM value.

Each axes are given the motion defined by a step function for P- Constant calibration. Motions repeated for different P – Constant values. Data collection during the P –Constant calibration is done 10 times for each axes in order to obtain phase average position data. Higher P - Constants cause overshooting position values on the other hand lower coefficients cannot catch the step function (Figure 12).

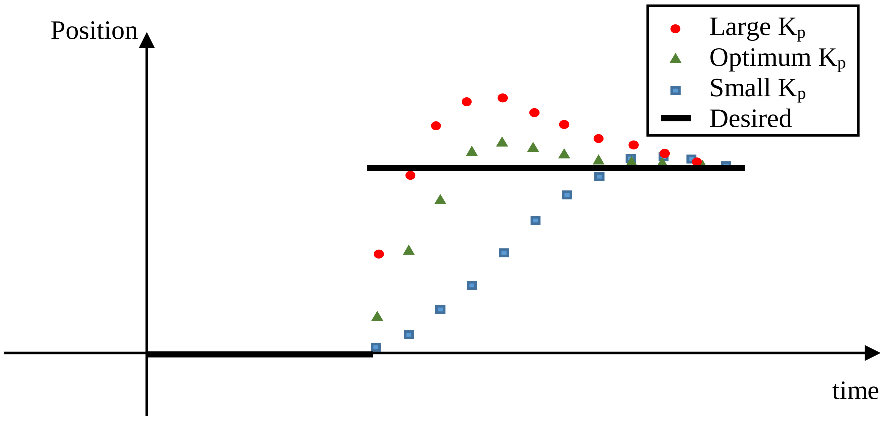

Figure 12 Step function motion response illustrations for different K_p

A step function motion, which have 30° of amplitude with 5 sec period, has used in order to determine the P – Constant characteristics of each axes. Only NACA 0006 wing model, which has 6 cm chord and 20 cm wing span, has used during the calibration test. Experimental Data for plunge axis is given on Figure 13.

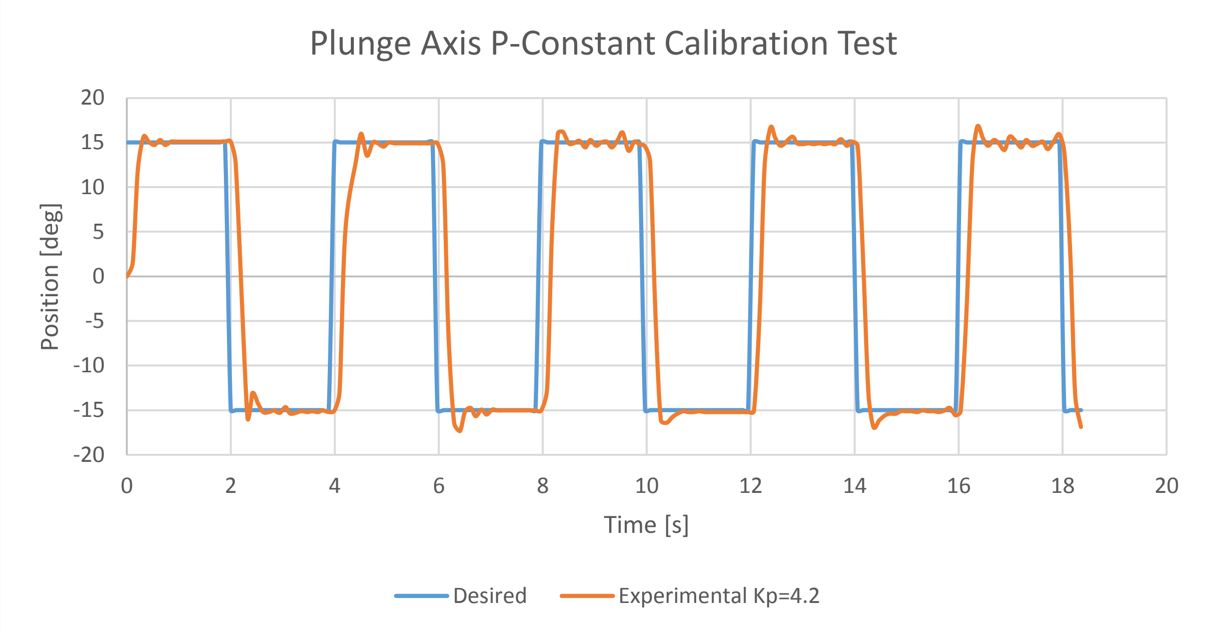

Figure 13 Plunge axis P-Constant calibration test data

Different proportional coefficients has been tested for calibration. At the end 4.2 proportional constant has been chosen as plunge axis P – Constant. During the plunge axis calibration test, only plunge axis is activated and the other two axis expected to be constant. However, pitch and yaw axis have position uncertainties. Pitch axis has larger uncertainty compared to yaw axis. Mean value and standard deviation of pitch axis position data are respectively 0.40 and 1.73 whereas yaw axis data are 0.13 and 0.10. Note that, Position uncertainties has negligible values for sinusoidal and ramp functions compared to step function motion trajectories. Calibration tests were performed for each axes and P – Constant of 4 obtain for pitch and yaw axes.

Minimum PWM value calibration has been done by using sinusoidal motion trajectory. Without any specified minimum PWM information, experimental position data cannot follow the sinusoidal trajectory especially around the peaks. A sinusoidal motion, which has 30° of amplitude and 5 sec period, has been used in calibration tests (Figure 14). Optimum minimum PWM value has been chosen as 20.

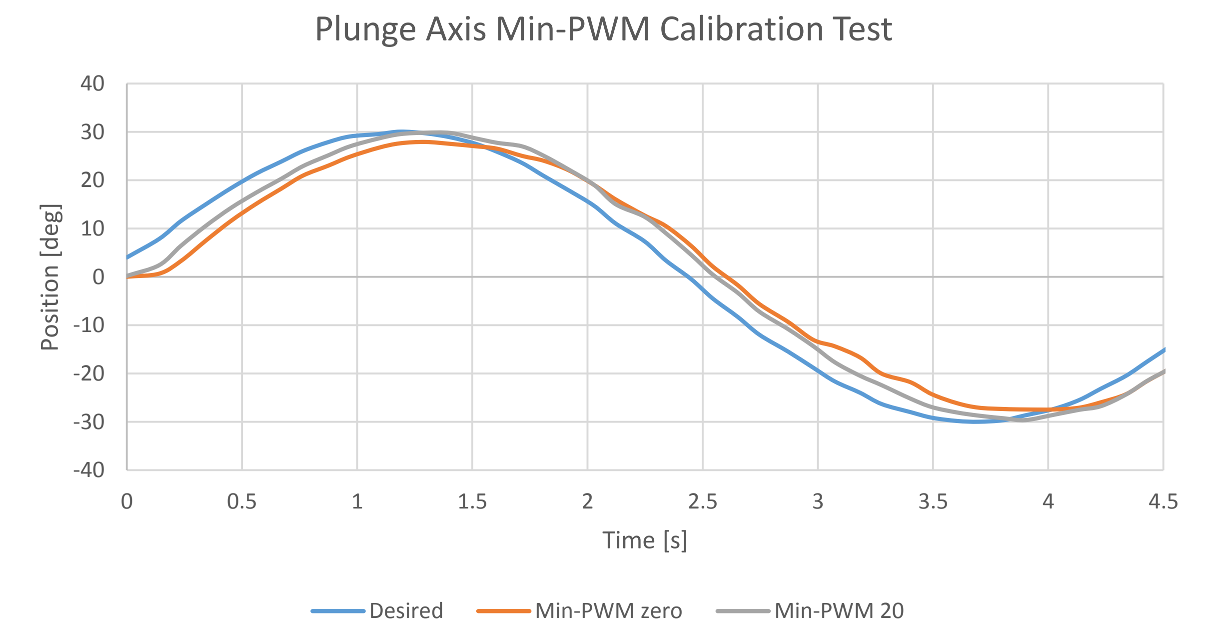

Figure 14 Plunge axis Min-PWM calibration test data

CONCLUSION

This paper mainly focus on design and calibration procedure of a novel-flapping wing mechanism. Adjustable kinematic of the mechanism enables the investigation of various flapping trajectories. Each wing has three degrees of freedom around pitch, plunge and yaw axes. That enables the investigation of 3-D flows around the flapping wings. Two wing model can be placed in tandem configuration and symmetric configuration. Flapping trajectories such as dragonfly's can be obtained by using tandem configuration. Furthermore, flapping trajectories similar to hummingbird and most of the insects can be created by symmetric or mono wing configuration. Modular structure of the wings enables a wide range of applications. Wings are controlled by special micro controllers by means of P-Control. Calibration of the wings has been done by optimizing the P-constant and minimum PWM value.

Future work will make characterization of the Robot-Wings. Also, ATI NANO 17 load cell, which has 6 degrees of freedom measurement ability, will be integrated to system. Hence, force and moment measurement in all three axes will be possible.

ACKNOWLEDGEMENT

TÜBA GEBİP Award given to Dr. Kurtuluş is greatly acknowledged (Award No: D.F.K/TÜBA-GEBİP/2012-18).

Special thanks to Emre Akgül and Serkan Tarçın for their efforts during design and production process.

References

J.M. Birch, M.H. Dickinson, *The influence of wing–wake interactions on the production of aerodynamic forces in flapping*, flight. J ExpBiol 206:2257–2272, 2003

J.M. McMichael, M.S. Francis*, Micro Air Vehicles-Toward a New Dimension in Flight*, Defense Advanced Research Projects Agency, TTO Document, 1996

H. Zheng, S. Schaeffer, R. McCauley and X. Deng*, "Aerodynamics of Dragonfly Flight and Robotic Design", in the Proceedings of IEEE International Conference on Robotics and Automation (ICRA'09), Pages 3666-3671, Kobe, Japan, May 2009.

M.H. Dickinson, K.G. Götz, *Unsteady aerodynamic performance of model wings at low Reynolds numbe*rs, J ExpBiol 174:45–64, 1993

R. G. George, M. B. *Colton, C. A. Mattson, S. L. Thomson, A Differentially Driven Flapping Wing Mechanism for Force Analysis and Trajectory Optimization*, International Journal of Micro Air Vehicles - Volume 4 - Number 1, March 2012

T. Weis-Fogh, *Quick estimates of flight fitness in hovering animals, including novel mechanism for lift production*. J ExpBiol 59:169–230, 1973